Impairment of the Transient Pupillary Light Reflex in *Rpe65*$^{-/-}$ Mice and Humans with Leber Congenital Amaurosis

Tomas S. Aleman,[1] *Samuel G. Jacobson,*[1] *John D. Chico,*[1] *Michele L. Scott,*[1] *Andy Y. Cheung,*[1] *Elizabeth A. M. Windsor,*[1] *Masatoshi Furushima,*[1] *T. Michael Redmond,*[2] *Jean Bennett,*[1] *Krzysztof Palczewski,*[3,4,5] *and Artur V. Cideciyan*[1]

Purpose. To determine the impairment of the transient pupillary light reflex (TPLR) due to severe retinal dysfunction and degeneration in a murine model of Leber congenital amaurosis (LCA) and in patients with the disease.

Methods. Direct TPLR was elicited in anesthetized, dark-adapted *Rpe65*$^{-/-}$ and control mice with full-field light stimuli (0.1 second duration) of increasing intensities (−6.6 to +2.3 log scot-cd · m^{-2}). 9-*cis*-Retinal was administered orally to a subset of *Rpe65*$^{-/-}$ mice, and TPLR was recorded 48 hours after the treatment. TPLR was also measured in a group of patients with LCA.

Results. Baseline pupillary diameters in *Rpe65*$^{-/-}$ and control mice were similar. TPLR thresholds of *Rpe65*$^{-/-}$ mice were elevated by 5 log units compared with those of control animals. The waveform of the TPLR in *Rpe65*$^{-/-}$ mice was similar to that evoked by 4.8-log-unit dimmer stimuli in control mice. Treatment of *Rpe65*$^{-/-}$ mice with 9-*cis*-retinal lowered the TPLR threshold by 2.1 log units. Patients with LCA had baseline pupillary diameters similar to normal, but the TPLR was abnormal, with thresholds elevated by 3 to more than 6 log units. When adjusted to the elevation of TPLR threshold, pupillary constriction kinetics in most patients were similar to those in normal subjects.

Conclusions. Pupillometry was used to quantify visual impairment and to probe transmission of retinal signals to higher nervous centers in a murine model of LCA and in patients with LCA. Mouse results were consistent with a dominant role of image-forming photoreceptors driving the early phase of the TPLR when elicited by short-duration stimuli. The objective and noninvasive nature of the TPLR measurement, and the observed post-treatment change toward normal in the animal model supports the notion that this may be a useful outcome measure in future therapeutic trials of LCA. (*Invest Ophthalmol Vis Sci.* 2004;45:1259–1271) DOI:10.1167/iovs.03-1230

Leber congenital amaurosis (LCA) is a group of hereditary retinal degenerations characterized by profound loss of visual function early in life.[1–2] Many genes causing LCA have been identified[1] (summarized in RetNet; http://www.sph.uth.tmc.edu/retnet; provided in the public domain by the University of Texas Houston Health Science Center, Houston, TX) and naturally occurring and genetically engineered animal models exist.[3–6] Recent success in restoration of visual function using oral retinoid[5] or gene therapy[6] has paved a preclinical path toward potential therapies in LCA. However, there are limited choices of objective measures of visual function that are equally applicable to infants, children, and adults with LCA, as well as to the animal models, due to the large operating range necessary to quantify the extremely severe abnormalities.

Light-induced contraction of the iris muscle depends on the integrity of multiple central nervous system (CNS) neurons involved in the well-known pupillary light reflex (PLR). Major signal input for this reflex originates from rod and cone (image-forming) photoreceptors in the outer retina as well as from intrinsically light-sensitive ganglion cells (non–image-forming [NIF] receptors) of the inner retina.[7] Information about ambient light level is conveyed through the afferent arc of the reflex, which includes retinal ganglion cells and their axonal projection toward pupillomotor centers in the CNS. Output signals travel back from those centers through the efferent arc of the reflex toward the ciliary ganglion, where the last synapse occurs and the last group of axons leaves the ganglion to innervate the iris muscle.[8,9]

The accessibility of the iris for observation provides an easy, noninvasive, and noncontact method to explore visual function through the study of the PLR. Abnormalities in the PLR have been described in human retinal degenerations as well as in animal models of these diseases,[6,10–15] and these earlier studies laid the groundwork for the present investigation. In the current work, we investigated the transient (as opposed to steady state) pupillary light reflex (TPLR) elicited by short duration stimuli as an objective and noninvasive measure of severe visual dysfunction in patients with LCA and other severe early-onset retinal degenerations, and in the *Rpe65* mouse model of one genetic form of these diseases.

Methods

Subjects

Mice. *Rpe65*$^{-/-}$ (n = 16) and *Rpe65*$^{+/+}$ (n = 7) mice (age 2–4 months) raised from birth in a 12-hour on-off cycle of dim (<3 lux) red

From the [1]Scheie Eye Institute, Department of Ophthalmology, University of Pennsylvania, Philadelphia, Pennsylvania; the [2]Laboratory of Retinal Cell and Molecular Biology, National Eye Institute, Bethesda, Maryland; and the Departments of [3]Ophthalmology, [4]Chemistry, and [5]Pharmacology, University of Washington, Seattle, Washington.

Supported by the National Institutes of Health Grants EY13385, EY13729, and EY13203; the Foundation Fighting Blindness (FFB); the Macula Vision Research Foundation; the Daniel Matzkin Research Fund; the Macular Disease Foundation; the F. M. Kirby Foundation; Research to Prevent Blindness (RPB); and the Paul and Evanina Mackall Trust. TSA is an FFB Career Development Awardee, KP is a RPB Senior Scientific Investigator, and AVC is an RPB William and Mary Greve Special Scholar.

Submitted for publication November 11, 2003; revised December 18, 2003, and January 5, 2004; accepted January 9, 2004.

Disclosure: **T.S. Aleman**, None; **S.G. Jacobson**, None; **J.D. Chico**, None; **M.L. Scott**, None; **A.Y. Cheung**, None; **E.A.M. Windsor**, None; **M. Furushima**, None; **T.M. Redmond**, None; **J. Bennett**, None; **K. Palczewski**, None; **A.V. Cideciyan**, None

The publication costs of this article were defrayed in part by page charge payment. This article must therefore be marked "*advertisement*" in accordance with 18 U.S.C. §1734 solely to indicate this fact.

Corresponding author: Artur V. Cideciyan, Scheie Eye Institute, 51 North 39th Street, Philadelphia, PA 19104; cideciya@mail.med.upenn.edu.

TABLE 1. Clinical Characteristics of the Patients with LCA

Patient	Age at Exam (y)	Gender	Visual Acuity*	Refraction†	Kinetic Visual Field (V-4e target)	Nystagmus
1	1	M	NP	+5.00‡	NP	Y
2§	1	M	NP	+6.00‡	NP	Y
3	2	F	NP	+6.00‡	NP	Y
4	5	F	6/200	+6.00‡	NP	Y
5	5	F	2/200	+6.00‡	Central island	Y
6	6	M	LP	NP	NP	Y
7‖	8	F	20/200	+0.75	Central island	N
8	9	M	20/100	−4.25	Central and temporal islands	Y
9	16	M	LP	+0.25	Temporal island	Y
10	17	M	LP	+10.00	Central island	Y
11	19	M	20/100	+1.50	Central island	Y
12	30	F	5/200	+8.00	Temporal island	Y
13	30	F	20/200	+8.00	Central and temporal islands	Y
14	33	F	3/200	−3.00	Central and temporal islands	Y
15	37	M	LP	−1.25	NM	Y
16	42	M	LP	+1.50	NM	Y
17	46	F	HM	+1.00	Central island	Y
18	59	F	LP	+4.00	NM	N

All patients had nondetectable full-field ERGs.[22] LP, light perception; HM, hand motions; NP, not performed; NM, not measurable.
* Best corrected visual acuity.
† Spherical equivalent.
‡ With cycloplegia.
§ Joubert syndrome; all other patients had uncomplicated LCA.
‖ *GUCY2D* mutation.[23] Other patients were of unknown genotype.

light were used in the pupillometry experiments. Animals were dark-adapted overnight and anesthetized intraperitoneally with a mixture of ketamine (45 mg/kg) and xylazine (17 mg/kg). Their body temperature was maintained on a heating pad. In pilot experiments, unanesthetized (restricted) animals showed an increase in pupillary fluctuation, making it more difficult to discern threshold responses. The anesthetic regimen used provides moderate sedation ensuring stable recordings. Anesthesia-induced miosis[13,16–18] was not observed. Our baseline dark-adapted pupil diameters (see the Results section) were comparable to those reported by others in unanesthetized[19,20] and anesthetized[21] mice. In a subset of *Rpe65*$^{-/-}$ mice (n = 8), 9-*cis*-retinal was administered by gavage, as described.[5] PLR was recorded before and 48 hours after the oral *cis*-retinoid. All studies were conducted in accordance with the ARVO Statement for the Use of Animals in Ophthalmic and Vision Research and were approved by the Institutional Review Board.

Human Studies. Patients with LCA (n = 18; see Table 1 for clinical characteristics) underwent complete eye examinations and visual function tests, as described.[24] Informed consent was obtained from subjects (or their parents) after explanation of the procedures. All studies conformed to the tenets of the Declaration of Helsinki and were approved by the Institutional Review Board.

Pupillometry

Instrumentation and Technique. The pupil was imaged with an infrared-sensitive video camera (LCL-903HS; Watec America Corp., Las Vegas, NV) and a macro zoom lens (MLH-10X; CBC, Ltd., Tokyo, Japan). The camera was centered on the equator of a 150-mm diameter sphere internally coated with white reflective paint. On the opposite side, along the optical axis of the video camera, a port was placed for the experimental pupil (Fig. 1A). For mouse experiments, the port was a circular 25-mm hole. For human experiments, the port was a rounded triangular hole with 70-mm sides (to clear the nose for right and left eye testing), and the pupil was placed at the apex of this port. Magnification of the pupil image was adjusted to achieve a baseline pupil diameter of 30% to 50% of the video height. A calibrated artificial pupil (2 or 6 mm in diameter for mouse and human studies, respectively), placed in the plane of the pupil before and after each experiment, provided a record of the exact magnification. Illumination for imaging in the dark was provided by infrared (940 nm) LEDs placed off-axis. A long-pass filter (Wratten 87B; Eastman Kodak, Rochester, NY) placed between the lens and the camera blocked wavelengths shorter than 800 nm (i.e., the stimuli used) from reaching the video record.

Two collars placed above the spherical Ganzfeld held offset ends of a bifurcated fiber-optic cable which provided the full-field light stimuli for recording the direct TPLR (i.e., transient changes in pupil size were measured in the same eye as was stimulated by light, and the contralateral eye was protected from light). An externally placed custom-built light source (100 W bulb, M28; Thorn Lighting Group, Manchester, UK) contained a collimating lens and a series of filters to define the spectral content and intensity of the stimulus. An electromechanical shutter (VS25S1T1; Vincent Associates, Rochester, NY), controlled by a shutter driver (T132; Vincent Associates, Rochester, NY), defined the onset and duration of the stimulus. In all experiments, stimulus duration was shorter than the onset of pupillary contraction to avoid changes in retinal illuminance superimposed on the kinetics of the response.

The video output from the camera was fed into a video timer (VS-50; Horita, Mission Viejo, CA), which inserted a date and time stamp near the upper border, and elapsed time from the last stimulus near the lower border of each video frame. The resultant video was fed into two computers for analysis of transients and a VCR (HR-S4800U; JVC, Yokahama, Japan) for continuous recording. One of the computers contained a digital image processor (RK-706PCI ver. 3.55; Iscan, Inc., Burlington, MA), which sampled the horizontal pupil diameter at 60 Hz. The second computer contained a video digitizer (PIXCI SV4 board, ver. 2.1; Epix, Inc., Buffalo Grove, IL) which produced a video sequence. The shutter, the video timer, and both computers were synchronized to the timing of each trigger released manually by the experimenter watching the pupil on a monitor screen covered by a deep red filter. Each record thus triggered was 5.7 seconds long, with a 1-second prestimulus baseline; however, records of any length could be obtained from the videotape record. Representative samples from digitized video sequences are shown in Fig. 1C for normal mouse and human eyes.

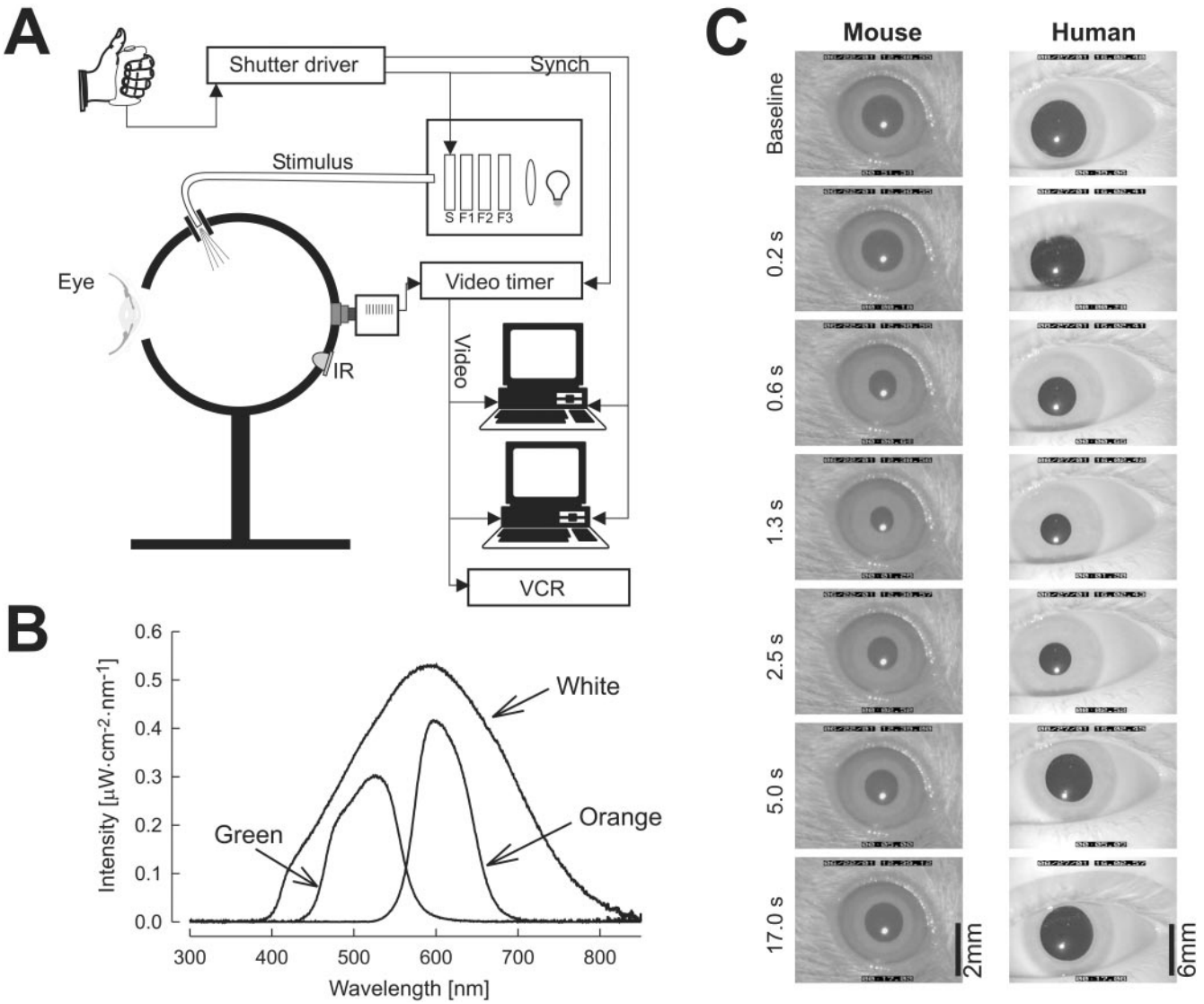

FIGURE 1. Summary of TPLR technique. (**A**) Schematic of pupillometer (components not drawn to scale) showing the stimulation, imaging, and recording components. (**B**) Spectral intensity distribution of stimuli used in the current work (maximum available white, green, and orange) measured at the plane of the cornea. (**C**) Video frames showing the appearance of the pupil at baseline and at different times after the light stimulus (2.3 log scot-cd · m^{-2}, 0.1 second) in a representative *Rpe65*$^{+/+}$ mouse and a normal human subject (age, 9 years). The video timer inserts date and time near the top and elapsed time from the last stimulus near the bottom of each frame. Mouse and human pupils were imaged at different magnification.

We performed pilot experiments to determine the relationship between TPLR response amplitude and baseline pupil diameter. The response amplitude measured at 0.6 seconds (see TPLR analysis) was nearly invariant with baseline diameter, as long as baseline diameter was greater than 1.2 mm in mice and greater than 4 mm in humans. Therefore, all interstimulus intervals were chosen to achieve baseline diameters equal to or greater than those values. A subgroup of animals (*Rpe65*$^{+/+}$, $n = 6$; *Rpe65*$^{-/-}$, $n = 5$) had their pupils dilated pharmacologically (tropicamide 1% and phenylephrine 2.5%) to determine maximal pupil diameters.

For the human studies, pupillometry was performed after more than 40 minutes of dark adaptation. In older children and adults, a chin–forehead rest was used to adjust the location of the test eye. In infants and younger children, the pupillometer was held by the experimenter while the subject was seated comfortably in the lap of a parent. TPLRs were recorded from one eye with a 0.1-second stimuli. Increasing interstimulus intervals were used with increasing stimulus intensities, to allow the pupil diameter to recover.

Stimuli and Light Calibration. The main stimulus was green (03FIB006; Melles Griot, Irvine, CA) the intensity of which could be controlled over a dynamic range of 8.9 log units (Ganzfeld luminance range from −6.6 to +2.3 log scot-cd · m^{-2}) with 0.1-log-unit resolution. In all experiments, green stimuli were presented from below threshold, progressively increasing in 1-log-unit steps. In some experiments, 0.5-log-unit steps were used near threshold to define better the luminance–response function. In addition orange (03FIB012; Melles Griot) stimuli were presented over a smaller dynamic range (−4.5 to +1.3 log scot-cd · m^{-2}) to determine spectral properties of mouse responses. In some experiments, a white stimulus (+2.5 log scot-cd · m^{-2}) was used to obtain the maximum response that could be elicited with this equipment. The luminances for all the stimuli were determined in three steps. First, the scotopic luminance of the maximum white stimulus was determined directly with a calibrated photometer (IL1700; International Light, Newburyport, MA) assuming mediation of responses by rods (described later). Second, the irradiance (at the

plane of the pupil) of the maximum intensities for the three types of stimuli was quantified with a calibrated spectrophotometer (USB2000; Ocean Optics, Dunedin, FL), and the relative efficiencies for rod photoreceptor stimulation were determined using the scotopic efficiency curve V'_λ for humans or using the rod response curve, which was the V'_λ curve corrected for human preretinal absorption, for mice (which have much more transparent lenses than do humans at short wavelengths).[25] The relative shift for the green and orange stimuli was less than 0.1 log unit for the two curves used. Third, the relative attenuations of the steps used over the relevant dynamic ranges of the green and orange stimuli were calibrated with the photometer. Fig. 1B shows the irradiance of the three types of stimuli at the plane of the pupil. The luminance values can be converted to isomerizations in individual rod photoreceptors as follows. In adult *Rpe65*$^{+/+}$ mice with fully dilated pupils, a luminance of 1 scot-cd · s · m^{-2} has been estimated to result in 100 to 5000 isomerizations per rod, based on the specific assumptions made.[21,26,27] In normal adult humans with fully dilated pupils, the same luminance has been estimated to result in 250 to 430 isomerizations per rod.[28]

The possibility of mediation of responses by visual pigments other than rhodopsin was also considered. Action spectra were derived from visual pigment templates with maxima at 360, 480, 490, and 510 nm, corresponding to ultraviolet (UV)-sensitive cones, NIF receptors, rods containing isorhodopsin, and middle-wavelength-sensitive (M) cones, respectively (see the Discussion section), and multiplied by the stimulus spectra to estimate relative effectiveness of the different stimuli. According to this analysis, mediation by UV cones, NIF receptors, and isorhodopsin would be expected to increase the green stimulus effectiveness by 1.5, 0.52, and 0.25 log units, respectively, and mediation by M-cones would be expected to decrease the green stimulus effectiveness by 0.23 log units compared with the orange stimulus.

TPLR Analysis. Baseline pupil diameter was defined as the average diameter during the 0.1 second immediately preceding the onset of each stimulus. TPLR response was defined as the difference between the pupil diameter measured at the fixed time after onset of light stimulus and at baseline. Response was negative for pupillary contraction and positive for pupillary dilation. Response amplitude was defined as the absolute value of pupil response, so that luminance–response functions had a conventional appearance (larger responses upward). Peak response refers to the difference in pupil diameter measured at the trough of the response and the baseline pupil diameter. In human studies, artifacts resulting from blinks were excluded from the analysis. Spontaneous changes in pupil diameter, or pupillary noise,[29] ultimately limit the detection sensitivity of pupillary responses near threshold. We determined the magnitude of these spontaneous oscillations in pupil diameter from the 1-second-long prestimulus baseline data we collected. These oscillations had amplitudes of 0.05 ± 0.01 mm in mice (2.5% ± 0.5% of prestimulus pupillary diameter) and 0.19 ± 0.06 mm in humans (2.1% ± 1.3% of baseline pupillary diameter). Similar values have been reported in rodents[21] and humans.[29–31] Response criteria of 0.1 mm for mice and 0.3 mm for humans were used in the current work to define threshold. All data are expressed (in text and in graphs) as the mean ± SEM, unless otherwise specified. The significance of the difference of group means was tested with Student's *t*-test (two-tailed, equal variance).

Results

Transient Pupillary Responses in *Rpe65*$^{+/+}$ and *Rpe65*$^{-/-}$ Mutant Mice

TPLR evoked by a white (+2.5 log scot-cd · m^{-2}), short-duration (0.1 second), full-field stimulus presented in the dark to a representative dark-adapted *Rpe65*$^{+/+}$ mouse shows two phases of the response: the diameter of the pupil decreases from the prestimulus baseline of 2.2 to 1.7 mm during the fast-constriction phase (0.3–1.5 seconds), and the pupil diameter enlarges during the slower dilation phase. The latter may be further subdivided into faster (2–5 seconds) and slower (>5 seconds) components (Fig. 2A). Manual measurement of digitized video images postacquisition (symbols, Fig. 2A) and automatic measurements performed during the acquisition (lines, Fig. 2A) gave comparable results. The former method, although time-consuming, provides data on the complete pupil shape for the duration of each recording; the latter method provides horizontal pupil diameter for a duration of 4.7 seconds after stimulus. There were no obvious deviations from a circular pupillary shape during the experiments, and most of our analysis concentrated on the earliest phases of the response. Unless otherwise specified, the automatic method was used. TPLR evoked by the same stimulus in an *Rpe65*$^{-/-}$ mouse also showed the same phases, but the response amplitude was smaller at its peak, the dilation phase started more quickly, and the baseline pupil diameter was reached faster (24 seconds) than normal (>50 seconds).

The dependency of the time course and amplitude of the TPLR on the intensity and spectral content of the stimulus was evaluated (Figs. 2B, 2C). In the *Rpe65*$^{+/+}$ mouse, TPLR threshold occurred near −5 log scot-cd · m^{-2} for the green stimulus; the *Rpe65*$^{-/-}$ mouse showed an elevated threshold near 0 log scot-cd · m^{-2} (Fig. 2B). Increasing stimulus intensity led to an acceleration of the constriction phase, an increase in peak response amplitude, and a retardation of the dilation phase. Near threshold and at low intensities, the pupil rapidly redilated to its baseline diameter after a small transient contraction. At the highest intensities, a sustained pupil contraction was observed followed by a delayed and biphasic dilation phase (Figs. 2A, 2B). At any given intensity, the *Rpe65*$^{-/-}$ response was smaller in amplitude and faster in redilation than in the *Rpe65*$^{+/+}$ animal. TPLR evoked by scotopically matched green and orange stimuli produced comparable responses in both amplitude and kinetics during the constriction and dilation phases in both groups of mice (Fig. 2B).

The properties of the earliest phases of TPLR response families are better appreciated on expanded axes (Fig. 2C). In the *Rpe65*$^{+/+}$ mouse, −5.7 log scot-cd · m^{-2} green stimulus did not evoke a response, but increasing intensities of green stimuli from −5.2 to +2.3 log scot-cd · m^{-2} elicited increasingly faster and larger amplitude TPLRs. The shape of the response (when normalized by amplitude) appeared invariant over the lower range of stimulus intensities. This invariance appeared to break down at the highest intensities in *Rpe65*$^{+/+}$ but not in *Rpe65*$^{-/-}$ mice (data not shown). Responses elicited with much higher intensity stimuli in the *Rpe65*$^{-/-}$ mouse showed properties similar to those evoked by lower intensities in the *Rpe65*$^{+/+}$ mouse. To quantify families of TPLRs in groups of mice, we parametrized the earliest phases of the response (Fig. 2C). Two parameters were defined to describe the response kinetics: the (first) time to reach criterion amplitude and the time to reach peak constriction. Three parameters were used to characterize response size: the amplitude at peak (maximum) constriction and the amplitude of constriction at fixed times of 0.6 and 2.5 seconds. The criterion response amplitude (see the Methods section), defined as 0.1 mm, corresponded to 5% of mean dark-adapted baseline pupil diameter and 15% of the mean maximum response in mice. The fixed time of 0.6 second was chosen to correspond to near midpoint on the leading edge. The fixed time of 2.5 seconds was chosen arbitrarily to be early enough in the recovery phase but longer than the peak times evoked by the brightest stimuli.

Quantitative TPLR Parameters in Mice

The pupil of dark-adapted *Rpe65*$^{+/+}$ mice had a diameter of 2.11 ± 0.13 mm (90% of the pharmacologically dilated pupil).

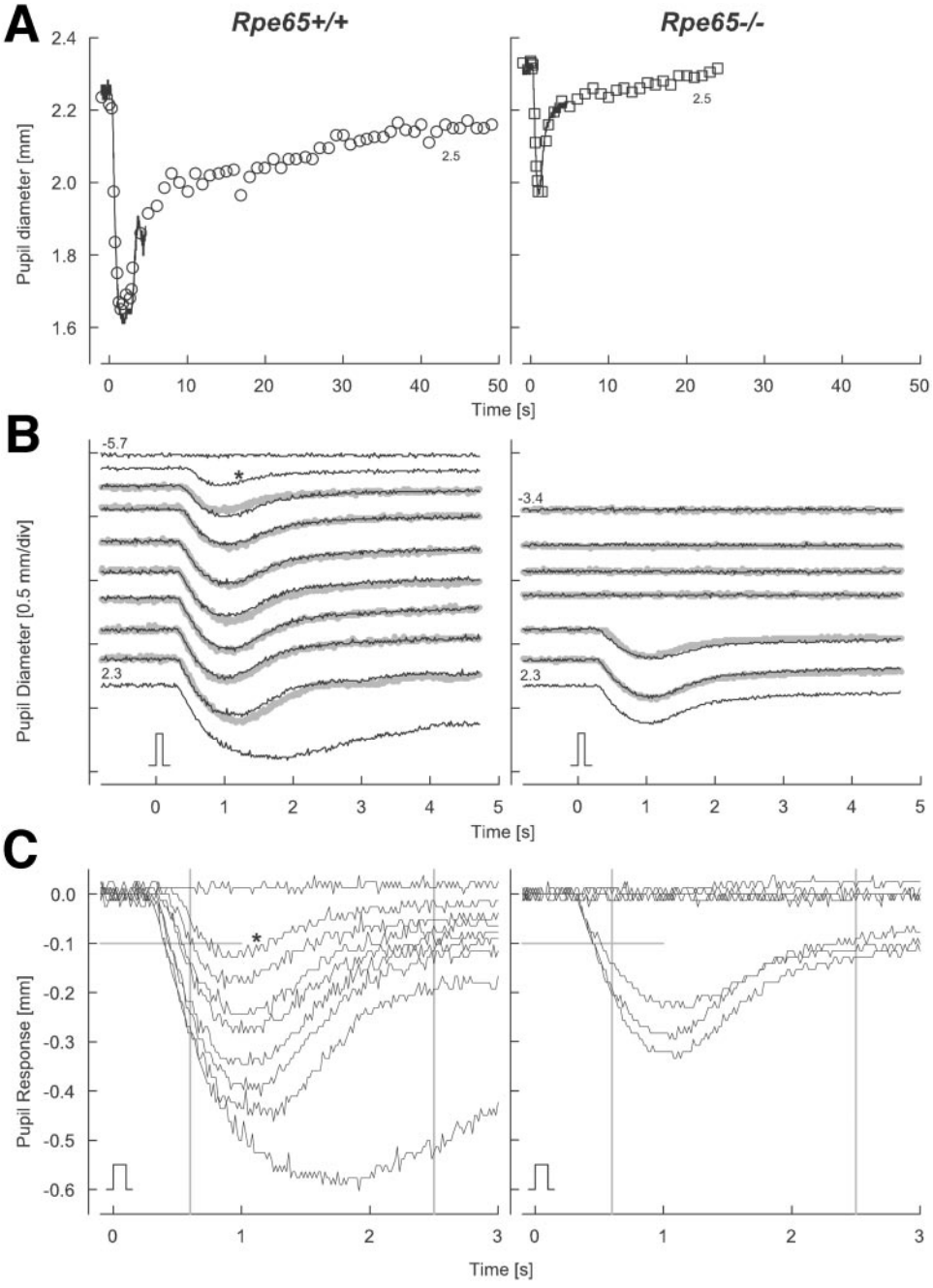

FIGURE 2. Representative TPLR data in wild-type (*Rpe65*$^{+/+}$) and mutant (*Rpe65*$^{-/-}$) mice. (**A**) Time course of constriction and dilation phases of the horizontal pupil diameter elicited by a 2.5 log scot-cd · m^{-2} white stimulus. Two types of measures are compared in each panel: manual analysis from individual video frames (*symbols*), and automatic analysis with an image-processing system (*lines*). (**B**) TPLR families elicited by green stimuli over the intensity range −5.7 to 2.3 log scot-cd · m^{-2} (*thin black traces*). Responses evoked by orange stimuli over the range of −4.5 to 1.3 log scot-cd · m^{-2} (*thick gray traces*) are shown overlapping green stimulus responses as pairs of matches. Stimulus steps were approximately 1 log unit. Intermediate steps were often used near threshold (✶). Zero time defined from the onset of the 0.1-second stimulus (stimulus monitor shown). (**C**) Response family evoked by green stimuli vertically shifted to equate prestimulus baselines shown on expanded horizontal and vertical axes. Some responses not shown for better visibility. *Gray vertical* and *horizontal lines*: criterion amplitude of 0.1 mm and fixed times of 0.6 and 2.5 seconds used for parameter extraction.

Criterion responses were reached at −4.88 ± 0.3 log scot-cd · m^{-2}. Thereafter, the pupil contracted with a TPLR latency, as defined by the time to reach criterion amplitude, that decreased monotonously from 0.51 ± 0.02 second at −4.7 log scot-cd · m^{-2} to 0.40 ± 0.01 second at +2.3 log scot-cd · m^{-2}. This parameter was nearly constant for the highest 4 log units of the intensity range (Fig. 3A). The other measure of TPLR kinetics, the time to peak response, was invariant near 1.0 ± 0.05 second over most of the available intensity range in *Rpe65*$^{+/+}$ mice, except at the highest two intensities, at which the peak response was increasingly delayed, occurring at 1.22 ± 0.03 seconds and 1.67 ± 0.14 seconds, respectively (Fig. 3B).

The dark-adapted pupil diameter of *Rpe65*$^{-/-}$ mice (2.23 ± 0.27 mm; 96% of the pharmacologically dilated pupil) was slightly larger than the dark-adapted pupil of *Rpe65*$^{+/+}$ mice, but this difference did not reach statistical significance (P = 0.34). Criterion responses were reached at +0.07 ± 0.09 log scot-cd · m^{-2}. Thereafter, the pupil contracted with a TPLR latency that, as in *Rpe65*$^{+/+}$, decreased monotonously from 0.50 ± 0.02 second at +0.4 log scot-cd · m^{-2} to 0.41 ± 0.01 second at +2.3 log scot-cd · m^{-2} (Fig. 3A). The time to peak response was constant near 0.97 ± 0.04 seconds in the *Rpe65*$^{-/-}$ mice, but, unlike *Rpe65*$^{+/+}$ mice, there was no delay of this parameter at the highest intensity (Fig. 3B). The latency parameters of *Rpe65*$^{-/-}$ mice could be made to correspond to those of the *Rpe65*$^{+/+}$ by shifting the data 4.4 log units to the left (not shown). Accordingly, the TPLR time to reach criterion responses at threshold was very similar in *Rpe65*$^{+/+}$ (0.55 ± 0.02 second) to that in *Rpe65*$^{-/-}$ mice (0.51 ± 0.02 second).

In *Rpe65*$^{+/+}$ mice, the earliest measured parameter of response size, TPLR amplitude at 0.6 second, showed a steep rise from threshold near −5.7 log scot-cd · m^{-2} to 0.17 ± 0.03 mm

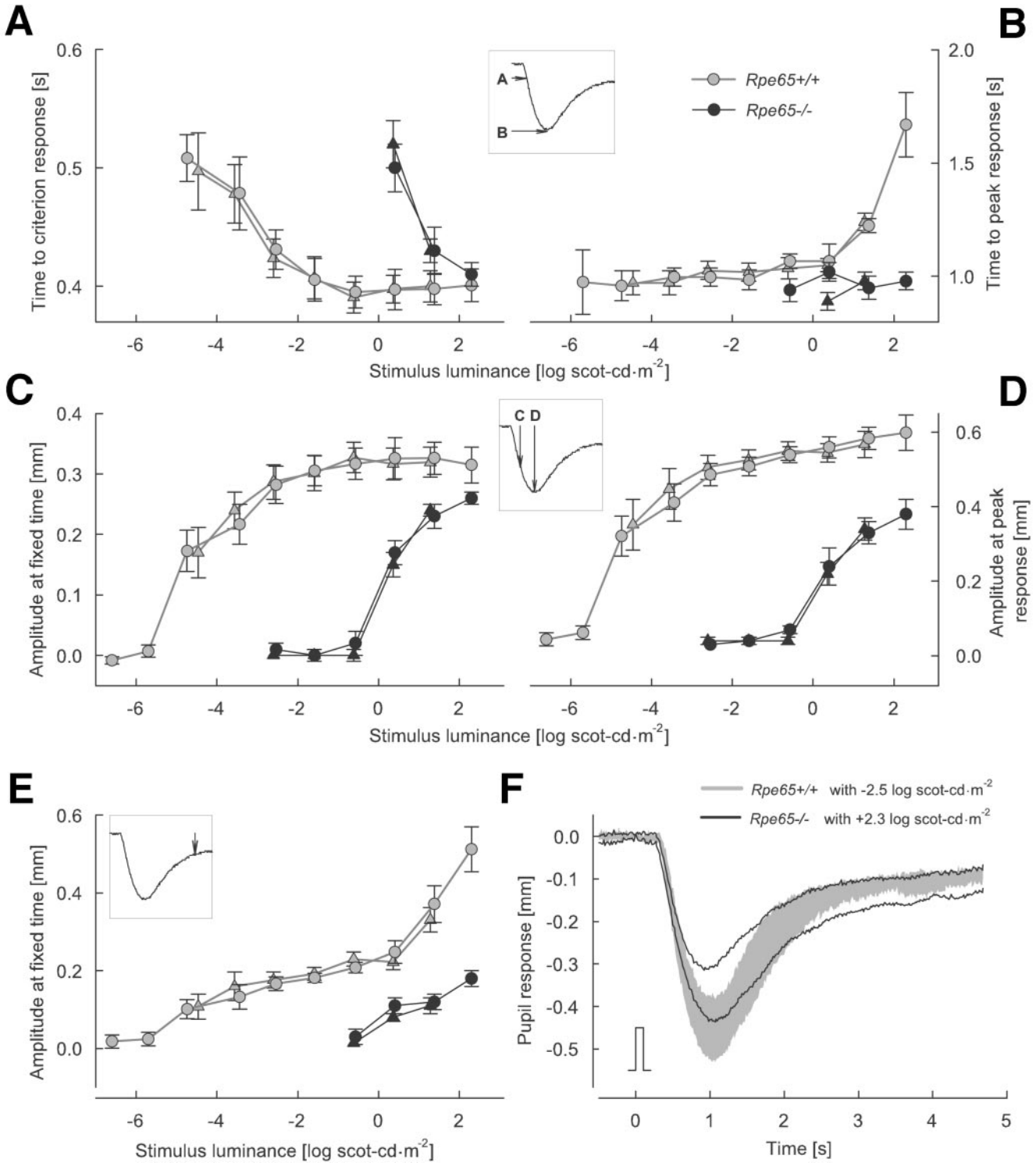

FIGURE 3. Parameters summarizing TPLR in *Rpe65*$^{+/+}$ and *Rpe65*$^{-/-}$ mice. (**A**, **B**) Latency of the response to reach criterion of 0.1 mm or peak amplitude. (**C**, **D**) Response amplitude measured at a fixed time of 0.6 second or at peak. (**E**) Response amplitude measured at a fixed time of 2.5 seconds. (**A–E**) *Circles* and *triangles*: green and orange stimuli, respectively. *Insets*: measurements on a representative TPLR. Error bars are ± SEM. (**F**) Comparison of responses (mean ± 2 SEM) elicited by a +2.3 log scot-cd · m^{-2} stimulus in the *Rpe65*$^{-/-}$ mice (*pair of traces*) with a −2.5 log scot-cd · m^{-2} stimulus in *Rpe65*$^{+/+}$ mice (*gray band*).

at −4.7 log scot-cd · m^{-2}. For the ensuing three log units (as the leading edge latency became progressively shorter; Fig. 3A), the amplitudes continued to grow with intensity, but at a much shallower rate than the rate observed near threshold (Fig. 3C). A saturated amplitude of 0.32 ± 0.03 mm was attained over the intensity range of −1.6 to +2.3 log scot-cd · m^{-2}. The peak amplitudes were larger than the amplitudes measured at 0.6 second, but the function relating them to luminance had a similar steep rise near threshold followed by a slower rate of rise (Fig. 3D). In *Rpe65*$^{-/-}$ mice, the two

response amplitude parameters showed some similarities to those in *Rpe65*$^{+/+}$ mice, although they were shifted to much higher stimulus intensities. The amplitude parameters of *Rpe65*$^{-/-}$ mice could be made to correspond nearly to the *Rpe65*$^{+/+}$ data by a 4.9-log-unit shift to the left (not shown). This shift corresponded closely to the difference in TPLR thresholds.

Early (≤0.6 seconds after stimulus onset) timing and amplitude measures with the green and orange stimuli (Figs. 3A, 3C) were well matched to the rhodopsin spectrum from −4.5 to −1.6 log scot-cd · m^{-2} in *Rpe65*$^{+/+}$ mice and from −0.6 to +1.3 log scot-cd · m^{-2} in *Rpe65*$^{-/-}$ mice. There was no evidence of a pigment spectrally different from rhodopsin contributing to TPLR. In *Rpe65*$^{+/+}$ mice, saturation of the timing and amplitude measures for stimuli higher than −1.6 log scot-cd · m^{-2} made it difficult to rule out a contribution by a different pigment at early times. At peak response, a small (~0.3 log) enhancement of the orange stimulus effectiveness was apparent in *Rpe65*$^{+/+}$ mice from −3.6 to −1.6 log scot-cd · m^{-2} (Fig. 3D) consistent with a contribution by mouse M-cones.

The early-dilation phase of the TPLR was quantified with the response amplitude measured at 2.5 seconds. This parameter showed a similar pattern of increase with stimulus intensity as the other two amplitude measures over the range of −4.7 to +0.4 log scot-cd · m^{-2} in *Rpe65*$^{+/+}$ mice. At the highest two intensities (corresponding to the increased latency of the peak response, Fig. 3B) the amplitude at 2.5 seconds grew steeply (Fig. 3E) in correspondence with the observed dramatic retardation of dilation kinetics (Fig. 2C). The amplitude-versus-luminance function in *Rpe65*$^{-/-}$ mice corresponded to the lower intensity portion of *Rpe65*$^{+/+}$ results. A shift of 4.9 log units to the left caused overlap of both functions. Amplitudes evoked with green and orange stimuli were in general well matched to the rhodopsin spectrum. At +1.3 log scot-cd · m^{-2} there was a small (~0.2 log) enhancement of the green stimulus effectiveness consistent with a possible contribution by NIF receptors.

With the five descriptive parameters of TPLR used in the current work, a response elicited in *Rpe65*$^{-/-}$ mice should be similar to a response elicited in *Rpe65*$^{+/+}$ mice with a stimulus that is 4 to 5 log units dimmer. This hypothesis was further tested by comparing the mean TPLR evoked by a −2.5-log scot-cd · m^{-2} green stimulus in *Rpe65*$^{+/+}$ mice with that evoked by a +2.3-log scot-cd · m^{-2} green stimulus in *Rpe65*$^{-/-}$ mice (Fig. 3F). The resultant TPLRs had very similar shapes with the mean value of *Rpe65*$^{-/-}$ results showing somewhat smaller peak amplitude compared with *Rpe65*$^{+/+}$ results. There was extensive overlap when the variability of the responses is considered. Thus, we conclude that the neural circuitry driving TPLR in *Rpe65*$^{-/-}$ mice is acting as if experiencing the ambient light levels through a 4.8-log-unit neutral density filter.

Acute Changes in Retinal Function Due to Treatment in *Rpe65*$^{-/-}$ Mice

Do TPLR parameters reflect acute changes in retinal function in individual animals? Previous work has shown that rod photoreceptor function of *Rpe65*$^{-/-}$ mice can be dramatically improved in the short-term by oral administration of 9-*cis*-retinal.[5,32] TPLR of *Rpe65*$^{-/-}$ mice also showed dramatic improvement 48 hours after oral administration of 9-*cis*-retinal. The family of responses elicited with increasing intensities of green stimulus in a representative *Rpe65*$^{-/-}$ mouse before and 48 hours after the treatment demonstrate the lower thresholds, larger amplitudes, and greater retardation of the dilation phases observed (Fig. 4A). The reproducibility of the treatment effect is demonstrated in four additional mice with the green stimulus of −0.6 log scot-cd · m^{-2}. In each animal, there was a definite response after treatment, compared with no response before treatment at this intensity (Fig. 4B). *Rpe65*$^{-/-}$ mice 48 hours after 9-*cis*-retinal administration had significantly ($P < 0.05$) lower TPLR thresholds (−2.05 ± 0.26 log scot-cd · m^{-2}) and larger maximum response amplitudes (0.59 ± 0.06 mm) compared with untreated *Rpe65*$^{-/-}$ mice (Fig. 4C). It is important to note that TPLR thresholds after treatment remained significantly ($P < 0.05$) elevated by 2.8 log units compared with those in *Rpe65*$^{+/+}$ mice (Fig. 4C).

TPLR in Normal Human Subjects and Patients with LCA

We extended the studies of the TPLR from mice to normal human subjects ($n = 8$; age range, 9–55 years) and patients with LCA ($n = 18$; age range, 1–59 years). Table 1 provides clinical details of the patients studied. Figure 5A compares TPLR elicited by a white stimulus (+2.5 log scot-cd · m^{-2}) in a representative, dark-adapted, normal subject and in patient 11. In the normal subject (Fig. 5A), presentation of the stimulus is followed by pupillary constriction starting at 0.28 seconds. From a prestimulus baseline diameter of 5.5 mm, the pupil diameter rapidly decreased during the fast-constriction phase (0.28–1 second) and reached its smallest diameter (3 mm) and remained constricted until 2 seconds when the dilation phase ensued. In the patient (Fig. 5A), constriction started at 0.3 second from a similar dark-adapted diameter, and the response progressed at a shallower rate, reaching its smallest diameter (4.1 mm) at 0.85 second. This resulted in a response amplitude that was approximately half of normal. Thereafter, the pupil started to redilate toward baseline.

Families of TPLR responses elicited with a range of green stimuli in a representative normal subject are shown for comparison with those from two patients with LCA (Fig. 5B). In the normal subject (Fig. 5B), the shape of the TPLR response family showed both similarities to and differences from the normal mouse responses previously described (Fig. 2B). The human TPLR threshold was near −5 log scot-cd · m^{-2}. In some subjects, the dilation phase transiently overshot the baseline at stimulus intensities near threshold. With increasing stimulus luminance there was an increase in amplitude, shortening of the latency to criterion response, and retardation of the dilation phase. At the highest intensities, a sustained pupil contraction is observed followed by a delayed and biphasic dilation phase, reminiscent of the mouse response. Response families in two patients with LCA illustrate the abnormalities encountered (Fig. 5B). In Patient 11, the TPLR threshold response was elevated by 3 log units, near −2 log scot-cd · m^{-2}. Responses above threshold were slower and shallower than normal responses. As stimulus intensity increased, there was an increase in amplitude, shortening of the latency to criterion response and retardation of the dilation phase. At the highest intensity (+2.3 log scot-cd · m^{-2}) TPLR response amplitude reached 50% of normal. Note that at any given stimulus intensity, responses in the patient resembled normal responses evoked by 3- to 4-log-unit dimmer stimulus. In patient 17 there was even greater threshold elevation (by at least 5 log units; near +1.4 log scot-cd · m^{-2}). TPLRs were elicited only at the highest two intensities and were very small in amplitude, with waveforms resembling normal responses near threshold. With increasing light intensity, there was a modest increase in response amplitude, which reached, at the highest intensity, only 10% of the normal amplitude. Results from these two patients indicate that loss of sensitivity may explain, at least in part, the differences in TPLR between LCA and normal subjects.

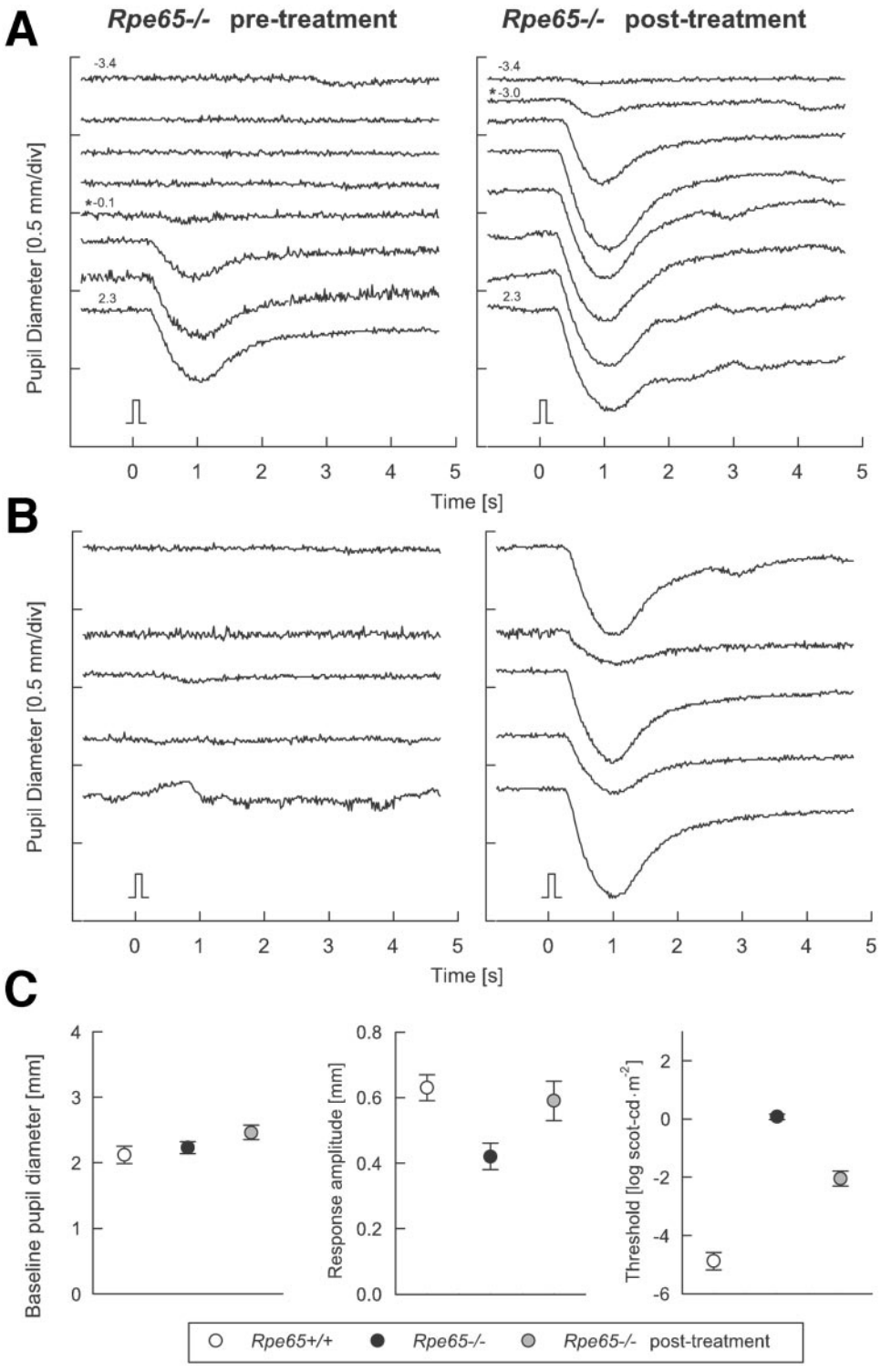

FIGURE 4. Effect on TPLR of treatment in *Rpe65*$^{-/-}$ mice. (**A**) Response families elicited with a range of green stimuli in an *Rpe65*$^{-/-}$ mouse before treatment and 48 hours after treatment with oral 9-*cis*-retinal. Intensity steps are approximately 1 log unit, except near response threshold (⋆). (**B**) Pre- and 48-hour posttreatment responses to a single-intensity (−0.6 log scot-cd · m^{-2}) green stimulus in four *Rpe65*$^{-/-}$ mice (in addition to the animal shown in **A**). (**C**) TPLR parameters in groups of *Rpe65*$^{-/-}$ mice before and after treatment (*Rpe65*$^{+/+}$ data also shown for comparison).

Quantifying the TPLR in Humans

Parameters for human TPLR were chosen to correspond closely to those used in mice and included baseline pupil diameter, the luminance (threshold) and time (latency) required to reach criterion amplitude, and the amplitude of constriction at a fixed time of 0.6 second. We analyzed the earliest portions of the response, because TPLR in patients (especially in young children) became less reliable with time after stimulus. Manual pupillary measurements complemented automatic measurements (Fig. 5A, open circles) in those patients with a greater degree of eye movement abnormality.

Pupil response amplitude (measured at 0.6 second) plotted as a function of stimulus luminance in this group of patients is compared with a mean normal function (Fig. 5C). The shape of the functions describing response amplitude parameters in normal human subjects (Fig. 5C) differed from that in the normal mouse. Instead of the steep increase in amplitude in the mouse luminance response function, the human TPLR amplitude at 0.6 seconds showed a gradual increase for approxi-

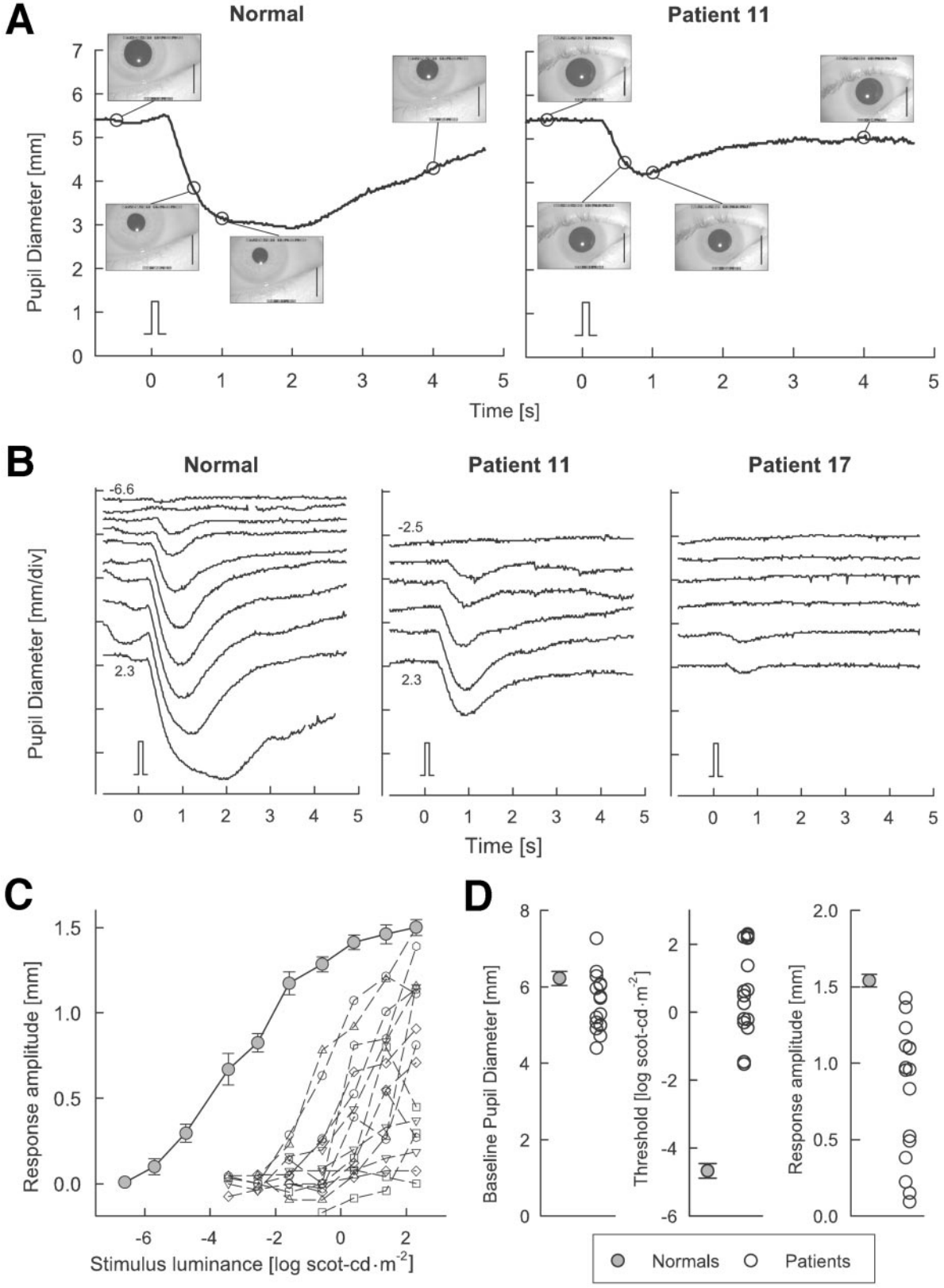

FIGURE 5. TPLR in normal humans and patients with LCA. (**A**) Time course of constriction and dilation phases of the horizontal pupil diameter elicited by a 2.5-log scot-cd · s · m^{-2} white flash (0.1 second, stimulus monitor shown) in a representative normal subject and in patient 11. *Symbols*: photographs of pupils of various diameters extracted manually from digitized video frames. Scale bars, 6 mm. (**B**) TPLR families elicited by green stimuli over the intensity range −6.6 to +2.3 log scot-cd · m^{-2} in a normal subject and two patients. Stimulus steps were approximately 1 log unit. (**C**) Individual luminance response functions measured at the fixed time of 0.6 seconds in all patients (*unfilled symbols*) compared with mean data for normal subjects (*filled circles*). (**D**) Distribution of baseline dark-adapted pupil diameter, TPLR threshold to criterion response, and maximum response in all patients compared with mean normal data.

mately 3 log units, from 0.11 ± 0.05 mm at −5.7 log scot-cd. m^{-2} to 1.2 ± 0.07 mm at −1.6 log scot-cd · m^{-2}. Thereafter, amplitudes continued to grow at a slower rate, reaching a 1.5 ± 0.03 mm (75% of baseline dark-adapted pupil diameter) at +2.3 log scot-cd · m^{-2}. There was a wide range of abnormalities in the patients. TPLR response functions in the patients were shifted toward higher luminances, showing greatly elevated thresholds and smaller response amplitudes. TPLR was recordable in 17 or 18 patients with the highest luminance stimulus. TPLR latency decreased monotonously with increasing stimulus intensities in both normal subjects and patients (data not shown). In normal subjects, mean TPLR response latency decreased from 0.6 ± 0.03 second at −5.7 log scot-cd · m^{-2} to 0.3 ± 0.01 second at the highest two intensities. In the patients, mean latency decreased from 0.58 ± 0.01 second at −1.58 log scot-cd · m^{-2} to 0.42 ± 0.07 second at the highest intensity. A clear saturation of this parameter was not observed in most patients. Averaged response amplitude and latency functions from patients nearly overlap the corresponding normal functions, by shifting them to the left along the horizontal axis by 4 log units. Response parameters are further summarized in Figure 5D. Baseline dark-adapted pupil diameter in normal subjects (6.2 ± 0.18 mm) was similar to that in patients (5.6 ± 0.2 mm). Patients showed elevated TPLR thresholds ranging from −1.53 to +2.3 log scot-cd · m^{-2} (normal, −4.67 ± 0.22 log scot-cd · m^{-2}) and reduced maximum response amplitude (0.6 ± 0.1 mm; range, 0.1–1.2 mm) to 40% of normal subjects (1.53 ± 0.04 mm).

Discussion

The severe visual impairment in most patients with early-onset retinal degenerations like LCA is difficult to quantify with conventional clinical instrumentation[33]; but, in the past, there has been no necessity to be exceedingly quantitative. Recently, preclinical success in animal models of LCA and the prospect of future clinical trials in certain severe retinal diseases[5,6] has made it worthwhile to explore clinically feasible methods that could precisely quantify the visual function of these patients. In the current work, we studied the time-honored clinical examination technique of pupillometry—more specifically, the properties of TPLR elicited with short-duration stimuli, to determine whether it had potential value as a surrogate measure of vision for future LCA clinical trials. We began with a murine model of LCA and found that the early phases of these objective responses are driven by the activity of classic image-forming photoreceptors and are altered toward normal by a treatment known to restore photoreceptor function in this model. Then, we explored the feasibility of the technique to quantify the visual abnormalities in patients with LCA.

Properties of the Direct TPLR in Normal Mice

TPLRs were exquisitely sensitive to light in dark-adapted *Rpe65*$^{+/+}$ mice. A conservative response threshold (0.1-mm constriction) was reliably reached with single (unaveraged) traces evoked by 0.1-second stimuli expected to cause approximately 1 isomerization per 250 murine rods. This response threshold was more sensitive than ERG b-wave thresholds[34] and somewhat less sensitive than scotopic threshold response (STR) and behavioral thresholds.[34,35] Thus, near threshold, the early phase of the mouse TPLR almost certainly is driven by the high amplification achieved in the rod phototransduction cascade, together with the temporal and spatial integration of rod signals through rod pathways of the distal and proximal retina. Demonstration of identical TPLR responses at early times evoked with chromatic stimuli matched for the rhodopsin spectrum (Figs. 2B, 3A, 3C) provided further support for mediation by the rod system near threshold. At later times and/or higher stimulus intensities (Figs. 3B, 3D, 3E), small additional contributions from mouse M-cones[36] or NIF receptors[37] could not be ruled out with the stimuli used in the current work.

The shape of mouse TPLR displayed an orderly continuum of change over the 9 log units of stimulus dynamic range provided by our instrumentation. Response latency to reach criterion amplitude became shorter over the first 5 log units, whereas the latency to reach peak constriction remained invariant. For the 3 log units of higher intensities, latency to peak became incrementally longer, consistent with a diminishing redilation component or growing delayed constriction component of the TPLR signal. The luminance–response function of the TPLR constriction amplitude showed a steep slope for the first log unit above threshold followed by a shallower slope at intermediate luminances. This unusual saturation function was essentially invariant for fixed early times (Fig. 3C) or at peak response (Fig. 3D), and it was suggestive of a form of incremental desensitization. Because the responses were normally recorded with increasing order of stimulus luminance, one may argue that increasing light adaptation of the retina may have desensitized the intermediate and high luminance portions of the function. This was not the case, however, because in pilot experiments TPLRs evoked with high luminance stimuli in fully dark-adapted eyes were nearly identical with TPLRs evoked with the same stimulus presented in the usual dim-to-bright order (data not shown). Of note, with steady state (or long stimulus duration) PLR measurements, luminance-response functions similar to the current work,[21] as well as those showing an apparently different shape,[37] have been described. Future studies are needed to define methodological and physiological parameters that may be contributing to the differences in saturation functions observed.

Consequences of Severe, Early Onset, and Retina-Wide Photoreceptor Dysfunction on the Murine TPLR

Young *Rpe65*$^{-/-}$ mice have nearly normal retinal structure with severely impaired but detectable photoreceptor function due to a block of the visual cycle.[4,5,38] As expected, *Rpe65*$^{-/-}$ mice showed severe impairment of the TPLR but threshold responses could readily be evoked with stimuli 4 to 5 log units brighter than normal. Spectral stimuli matched for rhodopsin absorption evoked identical responses at early (Fig. 3A, 3C) and peak times (Fig. 3D). At any given intensity of stimulation, TPLRs in *Rpe65*$^{-/-}$ differed from those in *Rpe65*$^{+/+}$ mice (Fig. 2). It is noteworthy that TPLRs of mutant mice could be reliably duplicated in *Rpe65*$^{+/+}$ mice by the addition of a 4.8-log-unit neutral-density filter in the stimulus light path (Fig. 3F). This difference in sensitivity to light was of the same order of magnitude as we observed in *RPE65*-mutant dogs compared with normal dogs.[6]

How did the level of desensitization of TPLR compare with other measures of visual dysfunction in the mutant mice? The activation phase of rod phototransduction in *Rpe65*$^{-/-}$ mice, as measured with ERG photoresponses in vivo, can be reproduced by a 1.6-log-unit reduction of the stimulus intensity.[5] Similarly, single rods from *Rpe65*$^{-/-}$ mice show normal activation and deactivation kinetics to subsaturating stimuli, as long as light intensities are reduced by 2.1 log units.[32] Both in vivo[5] and single-cell[32] experiments predict reduction of rod circulating current in the dark, although by somewhat different extents: 0.5 versus 0.9 log units, respectively. The activity of rod bipolar cells in *Rpe65*$^{-/-}$ mice, as estimated with ERG b-waves in vivo,[39] show a 3 to 4 log unit loss of sensitivity to light.[4,5,40] These results, taken together, suggest the existence of an additional ~1.5-log-unit loss of sensitivity between pho-

toreceptors and bipolar cells, and another ~1.5-log-unit loss of sensitivity between bipolar cells through the pupillary light reflex pathways. The origins and the accurate extents of these apparent losses are currently unknown, but it is tempting to speculate that there may be a contribution from synaptic abnormalities throughout the *Rpe65*$^{-/-}$ visual neural pathways subserving TPLR, possibly secondary to developmental lack of normal visual experience such as those described in mouse retina[41] and the rabbit ciliary ganglion[42] after visual deprivation. Consistent with this speculation are the TPLR results at 48 hours after oral 9-*cis*-retinal treatment. The retinoid treatment caused near complete recovery of photoreceptor function in *Rpe65*$^{-/-}$ mice,[5,32] but only a partial recovery of TPLR with a residual elevation of threshold response by 2.8 log units (Fig. 4).

The origin of the function in *Rpe65*$^{-/-}$ mice has been an enigma. Both rhodopsin and 11-*cis*-retinal are biochemically undetectable,[4,5,38,43] but rod-photoreceptor–mediated function is readily demonstrable.[5,40] Recently, it has been hypothesized that rod function in *Rpe65*$^{-/-}$ mice is driven by an endogenous supply of isorhodopsin, which has an absorption peak shifted toward shorter wavelengths compared with rhodopsin.[38] Mediation of TPLRs by isorhodopsin would correspond to approximately a 0.25-log-unit increase of the effectiveness of our green stimulus relative to the orange stimulus (shift of green results to the left relative to orange results in Figs. 3A–3E). There was no such tendency apparent in the early phase TPLR data of the current work. Future studies with more numerous and narrower-band stimuli are required to confirm the detailed action spectrum of the TPLR in *Rpe65*$^{-/-}$ mice. Also, it has recently been hypothesized that *Rpe65*$^{-/-}$ photoreceptors are effectively light adapted because of spontaneous activation of the phototransduction cycle by free opsin.[44] This would be expected[21] to cause a reduction in the pupil diameter of dark-adapted *Rpe65*$^{-/-}$ mice. Instead, mean dark-adapted pupil diameters of the *Rpe65*$^{-/-}$ mice in the present study were larger than those of *Rpe65*$^{+/+}$ mice, but this difference was not statistically significant (Fig. 4C). The pupil diameters of both groups did not differ from previously reported values.[21] If spontaneous activity of phototransduction in *Rpe65*$^{-/-}$ rods were confirmed, the lack of observed pupillary light adaptation could be postulated to originate from the desensitization of neural pathways driving the TPLR during early development by this "veiling light."

Contribution of NIF Photoreceptors to TPLR

A growing body of evidence supports the involvement of non-rod, non-cone photopigments in a network of intrinsically light-sensitive retinal ganglion cells that project to the suprachiasmatic nuclei and underlie NIF light responses.[7,45] It is thought that these cells provide signal input to the pupillary light reflex pathways through connections with the olivary pretectal nuclei.[46,47] Relatively late (>3 seconds after light onset) responses evoked by brighter stimuli appear to be dominated by NIF photoreceptors, whereas earliest responses evoked by dimmer stimuli are dominated by activation of rod and cone photoreceptors.[48,49] Our methods using near-threshold and short-duration stimuli and measuring transient responses at early times were designed to evaluate PLRs driven mostly by image-forming photoreceptors instead of sluggish NIF receptors.[50,51] Accordingly, we found 5-log-unit loss of TPLR sensitivity in *Rpe65*$^{-/-}$ mice instead of the 2-log-unit loss expected from longer duration stimuli if NIF photoreceptors were driving the pupil in the absence of image-forming photoreceptor function.[37,49] Furthermore, kinetics of the TPLR in *Rpe65*$^{-/-}$ mice support this notion with latencies (~0.4 seconds) approaching normal values in this study and normal rodent PLR latencies reported by others.[10,13,37] In contrast, pupillary light responses evoked by bright and long-duration light stimuli in mice with retinal degeneration have been reported to have much slower latencies.[37] In addition, NIF receptors have an action spectrum that is shifted by approximately 20 nm to shorter wavelengths than in the rhodopsin spectrum.[37] Our green and orange stimuli matched for rhodopsin absorption produced identical responses, thus providing support for the hypothesis that the early phase of the TPLRs evoked with short-duration stimuli used in the current work do not have major input from NIF receptors. At high intensities and late times (Fig. 3E), an NIF receptor contribution could not be ruled out. A comparison of pupil responses at later times evoked by short versus long duration stimuli in *Rpe65*$^{-/-}$ mice may be helpful to differentiate the responses driven by conventional versus NIF photoreceptors.

TPLR Abnormalities in Patients with LCA

Abnormal pupillary reactions are considered a feature of the clinical presentation of patients with LCA,[33,52] but few studies have quantified pupillary responses in these patients or others with hereditary outer retinal degenerations. With steady state stimuli, patients with retinitis pigmentosa, for example, can display PLR thresholds ranging from normal to a 5-log elevation. The extent of the elevation was greater in the group of patients without detectable full-field rod ERGs compared with the group with detectable ERGs, although there was an overlap.[12] In the present study, we extended our use of stimulus and analysis methods of TPLR, optimized to elicit a reflex driven by conventional photoreceptors in mice, to the study of normal human subjects and a group of patients with LCA.

The near-normal pupil diameters observed under dark-adapted conditions in our cohort of patients with LCA were consistent with previous results in patients with retinitis pigmentosa[53] and do not lend support to the hypothesized existence of spontaneous activation of the phototransduction cycle.[44,54] The pupils of all patients with LCA but one reliably responded to bright, short-duration light stimuli (Fig. 5D). Luminance–response functions showed varying degrees of threshold elevation ranging from 3 to more than 6 log units. Pupil response kinetics in 15 of 17 patients, once adjusted for threshold elevation, were similar to those of normal subjects, suggesting a primary role of loss of quantum catch at the photoreceptor level as the main underlying abnormality in this group of patients with LCA.

Threshold levels and waveform shapes of direct TPLRs evoked with short-duration full-field stimuli in normal dark-adapted human subjects were similar to those previously reported.[55–59] At all stimulus intensities used in the current work, constriction kinetics were faster than redilation kinetics[59,60] and the latency to criterion constriction appeared to saturate near 0.3 second. We chose to measure response amplitude in two different ways: at fixed early time and at peak constriction. Measuring at a fixed early time had the advantage of quantifying dominant signal components causing constriction with little intrusion from signal components causing redilation of the pupil. Furthermore, TPLR at early times is now believed to be driven by conventional (image-forming) photoreceptors,[48] and our mouse results support this notion. Measuring at peak time, on the other hand, allowed for delays in signal transmission as may be apparent in some patients, but the interpretation was complicated by greater involvement of redilation signals, possible abnormalities in more proximal neural circuits, or even involvement of signals driven by NIF photoreceptors, especially at higher luminance stimuli.

Use of TPLR as an Outcome Measure in Clinical Trials of LCA

In patients with severe hereditary retinal degenerations, the early phase of the direct TPLR with a short-duration stimulus is a convenient, objective, noninvasive, and noncontact test of visual function that may be a useful complement to other objective measures of vision (e.g., ERG and VEP). After an appropriate period of dark adaptation, TPLR measurements covering more than 8 log units of dynamic range above normal threshold were able to be performed in approximately 15 minutes. The full-field stimulus confronted the uncontrolled fixation difficulties and nystagmus common in this patient population and was especially useful in infants and young children with limited cooperation.[61,62] TPLR is temporally locked to the stimulus and thus allows for better differentiation of light-evoked changes in pupil size from fluctuations due to other reasons, as may occur with steady state PLR measures. How pupillary thresholds would relate to perceptual thresholds is currently an unanswered question in this severely impaired population of patients. In cooperative adult subjects, this question should be addressed. Modifications of the current instrument could permit simultaneous determination and comparison of thresholds for objective (TPLR) and subjective measures of vision,[55,63] such as has occurred in other groups of patients.[64] In normal human subjects, both rod and cone systems can contribute to the consensual pupillary light reflex with transient stimuli under certain experimental conditions.[65] Estimation of the type of photoreceptors mediating the direct TPLR responses in normal subjects and patients by determining the action spectra was not within the scope of the current work but is certainly a worthy future pursuit.

An outcome measure for human clinical trials attempting to modify the course of severe retinal degenerative disease must have a large dynamic range and, ideally, would be equally applicable to infants, children, and adults, as well as to the animal models used for preclinical studies. Our murine studies and results indicating feasibility of such measurements in patients with LCA suggest early phase of the TPLR elicited with short-duration stimuli may be a useful means to quantify photoreceptor-driven visual function transmitted through higher visual pathways.

Acknowledgments

The authors thank F. Letterio for assistance with optical and mechanical engineering and Sharon B. Schwartz, Elaine E. Smilko, Elaine deCastro, Ernest Glover, Mary Nguyen, Paul Schied, Vaibhav Bhuva, Anthony Nguyen, Alex Pantelyat, Matthew Batten, and J. Preston VanHooser for providing critical help with the studies.

References

1. Cremers FP, van den Hurk JA, den Hollander AI. Molecular genetics of Leber congenital amaurosis. *Hum Mol Genet*. 2002;11:1169–1176.
2. Fulton AB, Hansen RM, Mayer DL. Vision in Leber congenital amaurosis. *Arch Ophthalmol*. 1996;114:698–703.
3. Semple-Rowland SL, Lee NR, Van Hooser JP, Palczewski K, Baehr W. A null mutation in the photoreceptor guanylate cyclase gene causes the retinal degeneration chicken phenotype. *Proc Natl Acad Sci USA*. 1998;95:1271–1276.
4. Redmond TM, Yu S, Lee E, et al. Rpe65 is necessary for production of 11-cis-vitamin A in the retinal visual cycle. *Nat Genet*. 1998;20:344–351.
5. Van Hooser JP, Aleman TS, He YG, et al. Rapid restoration of visual pigment and function with oral retinoid in a mouse model of childhood blindness. *Proc Natl Acad Sci USA*. 2000;97:8623–8628.
6. Acland GM, Aguirre GD, Ray J, et al. Gene therapy restores vision in a canine model of childhood blindness. *Nat Genet*. 2001;28:92–95.
7. Foster RG. Keeping an eye on time. The Cogan Lecture. *Invest Ophthalmol Vis Sci*. 2002;43:1286–1298.
8. Loewenfeld IE. The light reflex. In: Loewenfeld IE, ed. *The Pupil: Anatomy, Physiology and Clinical Applications.* Ames, IA: Iowa State University Press; 1993:193–267.
9. Barbur JL. Learning from the pupil: studies in basic mechanisms and clinical applications. In: Chalupa LM, JS Werner. *The Visual Neurosciences.* Cambridge, MA: MIT Press; 2003:641–656.
10. Trejo LJ, Cicerone CM. Retinal sensitivity measured by the pupillary light reflex in RCS and albino rats. *Vision Res*. 1982;22:1163–1171.
11. Jiang MQ, Thompson HS. Pupillary defects in retinitis pigmentosa. *Am J Ophthalmol*. 1985;99:607–608.
12. Birch EE, Birch DG. Pupillometric measures of retinal sensitivity in infants and adults with retinitis pigmentosa. *Vision Res*. 1987;27:499–505.
13. Whiteley SJ, Young MJ, Litchfield TM, Coffey PJ, Lund RD. Changes in the pupillary light reflex of pigmented royal college of surgeons rats with age. *Exp Eye Res*. 1998;66:719–730.
14. Tan L, Kondo M, Sato M, Kondo N, Miyake Y. Multifocal pupillary light response fields in normal subjects and patients with visual field defects. *Vision Res*. 2001;41:1073–1084.
15. Bergamin O, Kardon RH. Greater pupillary escape differentiates central from peripheral visual field loss. *Ophthalmology*. 2002;109:771–780.
16. Clarke RJ, Ikeda H. Luminance and darkness detectors in the olivary and posterior pretectal nuclei and their relationship to the pupillary light reflex in the rat. I. Studies with steady luminance levels. *Exp Brain Res*. 1985;57:224–232.
17. Radel JD, Das S, Lund RD. Development of light activated pupilloconstriction in rats as mediated by normal and transplanted retinae. *Eur J Neurosci*. 1992;4:603–615.
18. Radel JD, Kustra DJ, Das S, Elton S, Lund RD. The pupillary light response: assessment of function mediated by intracranial retinal transplants. *Neuroscience*. 1995;68:909–924.
19. Mitchiner JC, Pinto LH, Vanable JW Jr. Visually evoked eye movements in the mouse (Mus musculus). *Vision Res*. 1976;16:1169–1171.
20. Semo M, Peirson S, Lupi D, Lucas RJ, Jeffery G, Foster RG. Melanopsin retinal ganglion cells and the maintenance of circadian and pupillary responses to light in aged rodless/coneless (rd/rd cl) mice. *Eur J Neurosci*. 2003;17:1793–1801.
21. Pennesi ME, Lyubarsky AL, Pugh EN Jr. Extreme responsiveness of the pupil of the dark-adapted mouse to steady retinal illumination. *Invest Ophthalmol Vis Sci*. 1998;39:2148−2156.
22. Jacobson SG, Yagasaki K, Feuer WJ, Roman AJ. Interocular asymmetry of visual function in heterozygotes of X-linked retinitis pigmentosa. *Exp Eye Res.* 1989;48:679–691.
23. Milam AH, Barakat MR, Gupta N, et al. Clinicopathologic effects of mutant GUCY2D in Leber congenital amaurosis. *Ophthalmology.* 2003;110:549–558.
24. Jacobson SG, Cideciyan AV, Aleman TS, et al. Crumbs homolog 1 (CRB1) mutations result in a thick human retina with abnormal lamination. *Hum Mol Genet*. 2003;12:1073–1078.
25. Dillon J, Zheng L, Merriam JC, Gaillard ER. The optical properties of the anterior segment of the eye: implications for cortical cataract. *Exp Eye Res*. 1999;68:785–795.
26. Goto Y, Peachey NS, Ziroli NE, et al. Rod phototransduction in transgenic mice expressing a mutant opsin gene. *J Opt Soc Am A*. 1996;13:577–585.
27. Hetling JR, Pepperberg DR. Sensitivity and kinetics of mouse rod flash responses determined in vivo from paired-flash electroretinograms. *J Physiol*. 1999;516:593–609.
28. Breton ME, Schueller AW, Lamb TD, Pugh EN Jr. Analysis of ERG a-wave amplification and kinetics in terms of the G-protein cascade of phototransduction. *Invest Ophthalmol Vis Sci*. 1994;35:295–309.
29. Stark LR. The pupil as a paradigm example of a neurological control system: mathematical approaches in biology. In: Loewen-

feld IE, ed. *The Pupil: Anatomy, Physiology and Clinical Applications.* Ames, IA: Iowa State University Press; 1993:630–647.
30. Longtin A, Milton JG, Bos JE, Mackey MC. Noise and critical behavior of the pupil reflex at oscillation onset. *Phys Rev A.* 1990;41:6992–7005.
31. Bitsios P, Szabadi E, Bradshaw CM. Comparison of the effects of venlafaxine, paroxetine and desipramine on the pupillary light reflex in man. *Psychopharmacology*. 1999;143:286–292.
32. Van Hooser JP, Liang Y, Maeda T, et al. Recovery of visual functions in a mouse model of Leber congenital amaurosis. *J Biol Chem*. 2002;277:19173–19182.
33. Fazzi E, Signorini SG, Scelsa B, Bova SM, Lanzi G. Leber's congenital amaurosis: an update. *Eur J Paediatr Neurol*. 2003;7:13–22.
34. Saszik SM, Robson JG, Frishman LJ. The scotopic threshold response of the dark-adapted electroretinogram of the mouse. *J Physiol*. 2002;543:899–916.
35. Herreros de Tejada P, Munoz Tedo C, Costi C. Behavioral estimates of absolute visual threshold in mice. *Vision Res*. 1997;37:2427–2432.
36. Jacobs GH, Neitz J, Deegan JF. Retinal receptors in rodents maximally sensitive to ultraviolet light. *Nature*. 1991;353:655–656.
37. Lucas RJ, Douglas RH, Foster RG. Characterization of an ocular photopigment capable of driving pupillary constriction in mice. *Nat Neurosci*. 2001;4:621–626.
38. Fan J, Rohrer B, Moiseyev G, Ma JX, Crouch RK. Isorhodopsin rather than rhodopsin mediates rod function in RPE65 knock-out mice. *Proc Natl Acad Sci USA*. 2003;100:13662–13667.
39. Pugh EN Jr, Falsini B, Lyubarsky AL. The origin of the major rod- and cone-driven components of the rodent electroretinogram and the effect of age and light-rearing history on the magnitude of these components. In: Williams TP, Thistle AB, eds. *Photostasis and Related Phenomena.* New York: Plenum Press; 1998:93–128.
40. Seeliger MW, Grimm C, Stahlberg F, et al. New views on RPE65 deficiency: the rod system is the source of vision in a mouse model of Leber congenital amaurosis. *Nat Genet*. 2001;29:70–74.
41. Tian N, Copenhagen DR. Visual stimulation is required for refinement of ON and OFF pathways in postnatal retina. *Neuron*. 2003;39:85–96.
42. Jackson PC. Reduced activity during development delays the normal rearrangement of synapses in the rabbit ciliary ganglion. *J Physiol*. 1983;345:319–327.
43. Qtaishat NM, Redmond TM, Pepperberg DR. Acute radiolabeling of retinoids in eye tissues of normal and rpe65-deficient mice. *Invest Ophthalmol Vis Sci*. 2003;44:1435–1446.
44. Woodruff ML, Wang Z, Chung HY, Redmond TM, Fain GL, Lem J. Spontaneous activity of opsin apoprotein is a cause of Leber congenital amaurosis. *Nat Genet*. 2003;35:58–64.
45. Berson DM. Strange vision: ganglion cells as circadian photoreceptors. *Trends Neurosci*. 2003;26:314–320.
46. Hattar S, Liao H-W, Takao M, Berson DM, Yau K-W. Melanopsin-containing retinal ganglion cells: architecture, projections, and intrinsic photosensitivity. *Science.* 2002;295:1065–1070.
47. Morin LP, Blanchard JH, Provencio I. Retinal ganglion cell projections to the hamster suprachiasmatic nucleus, intergeniculate leaflet, and visual midbrain: bifurcation and melanopsin immunoreactivity. *J Comp Neurol*. 2003;20:401–416.
48. Lucas RJ, Hattar S, Takao M, Berson DM, Foster RG, Yau KW. Diminished pupillary light reflex at high irradiances in melanopsin-knockout mice. *Science*. 2003;299:245–247.
49. Hattar S, Lucas RJ, Mrosovsky N, et al. Melanopsin and rod-cone photoreceptive systems account for all major accessory visual functions in mice. *Nature*. 2003;424:75–81.
50. Berson DM, Dunn FA, Takao M. Phototransduction by retinal ganglion cells that set circadian clock. *Science*. 2002;295:1070–1073.
51. Sekaran S, Foster RG, Lucas RJ, Hankins MW. Calcium imaging reveals a network of intrinsically light-sensitive inner-retinal neurons. *Curr Biol*. 2003;13:1290–1298.
52. Heckenlively JR. *Retinitis Pigmentosa.* Philadelphia: JB Lippincott Co.; 1988.
53. Berezovsky A, Salamao SR, Birch DG. Pupil size following dark adaptation in patients with retinitis pigmentosa. *Braz J Med Biol Res*. 2001;34:1037–1040.
54. Lisman J, Fain G. Support for the equivalent light hypothesis for RP. *Nat Med*. 1995;1:1254–1255.
55. Burke DW, Ogle KN. Comparison of visual and pupillary light thresholds in periphery. *Arch Ophthalmol*. 1964;71:400–408.
56. Ohba N, Alpern M. Adaptation of the pupil light reflex. *Vision Res*. 1972;12:953–967.
57. Ellis CFK. The pupillary light reflex in normal subjects. *Br J Ophthalmol*. 1981;65:754–759.
58. Heller PH, Perry F, Jewett DL, Levine JD. Autonomic components of the human pupillary light reflex. *Invest Ophthalmol Vis Sci*. 1990;31:156–162.
59. Bergamin O, Zimmerman MB, Kardon RH. Pupil light reflex in normal and diseased eyes: diagnosis of visual dysfunction using waveform partitioning. *Ophthalmology*. 2003;110:106–114.
60. Meyer ME, Ogle KN, Hollenhorst RW, Moyer NJ. Derivative curve in evaluation of the pupillary reflex response to light. *Exp Eye Res*. 1969;8:355–363.
61. Sugita K, Sugita Y, Mutsuga N, Takaoka Y. Pupillary reflex perimeter for children and unconscious patients. *Monogr Hum Genet*. 1972;6:199.
62. Banks MS, Munsinger H. Pupillometric measurement of difference spectra for three color receptors in an adult and a four-year-old. *Vision Res*. 1974;14:813–817.
63. Schweitzer NM, Bouman MA. Differential threshold measurements on the light reflex of the human pupil. *Arch Ophthalmol*. 1958;59:541–550.
64. Kardon RH, Kirkally PA Thompson HS. Automated pupil perimetry. Pupil field mapping in patients and normal subjects. *Ophthalmology*. 1991;98:485–496.
65. Alpern M, Campbell FW. The spectral sensitivity of the consensual light reflex. *J Physiol*. 1962;164:478–507.